Solar Phys (2010) 264: 353–364
DOI 10.1007/s11207-010-9585-5

Coronal Shocks Associated with Impulsive and Decaying Phases of Solar Flares

K. Suresh · S. Umapathy · A. Shanmugaraju · B. Vršnak

Received: 3 February 2010 / Accepted: 26 May 2010 / Published online: 30 June 2010

Abstract We have analyzed a set of 147 metric Type II radio bursts observed by Culgoora radio spectrograph from November 1997 to December 2006. These events were divided into two sets: The first subset contains Type II events that started during the impulsive phase of the associated solar flares and the second subset contains those starting during the decaying phase of flares. Our main aim is to differentiate the metric Type IIs, flares and coronal mass ejections (CMEs) of these two subsets. It is found that while Type II burst characteristics of both subsets are very similar, there are significant differences between flare and CME properties for these two subsets. Considering all analyzed relationships between the characteristics of Type IIs, flares and CMEs in these two Type II subsets, we conclude that most of the coronal shocks causing metric Type II bursts are driven by CMEs, but that a fraction of events are probably ignited by solar flares.

Keywords Coronal mass ejection · Solar flares · Solar radio bursts

1. Introduction

Many years of research have demonstrated that large, non-recurrent geomagnetic storms, shock-wave disturbances in the corona and solar wind, and energetic particle events in interplanetary space often occur in close association with coronal mass ejections (CMEs) and large solar flares. These two phenomena are the most energetic explosive processes in the solar system, having a direct effect on the Earth's magnetosphere and atmosphere. So, the

K. Suresh (✉) · S. Umapathy
School of Physics, Madurai Kamaraj University, Madurai, India
e-mail: suresh66066@yahoo.com

A. Shanmugaraju
Department of Physics, Arul Anandar College, Karumathur, Madurai, India

B. Vršnak
Hvar Observatory, Faculty of Geodesy, Kačićeva 26, 10000 Zagreb, Croatia

study of flares, CMEs, and the associated shock waves is the one of the most important subjects in the solar-activity research.

The CME/flare associated shock waves, revealed by the Type II solar radio bursts, have been studied by solar astronomers for more than 50 years. Utilizing the dynamic spectra of solar radio emission, Wild and McCready (1950) first revealed the existence of slowly-drifting bursts, which they denoted as Type II radio bursts. The characteristics of Type II bursts are summarized in Nelson and Melrose (1985), Mann, Classen, and Aurass (1995), Aurass (1997), and Gopalswamy (2000). The Type II emission is interpreted as the radio signature of a collisionless magnetohydrodynamic shock wave propagating throughout the solar corona (Uchida, 1960).

The shock waves can be caused either by flares or CMEs (Smerd, Sheridan, and Stewart, 1975; Gopalswamy *et al.*, 1998; Cliver, 1999; Vršnak and Cliver, 2008). In order to understand the association of Type IIs with flares and CMEs, many investigations have been recently made on solar eruptive events (see, *e.g.*, Reiner *et al.*, 2001; Gopalswamy *et al.* 2001a, 2001b). It is generally accepted that the interplanetary Type IIs are driven by CMEs (decameter-hectometic and kilometric Type IIs). On the other hand, the source of coronal Type IIs (metric range) is still under debate. For example, Vršnak *et al.* (1995) and Shanmugaraju *et al.* (2003) showed that the occurrence of most of metric Type IIs are closely temporally related to the peak time of flares. Recently, Shanmugaraju *et al.* (2005) and Subramanian and Ebenezer (2006) investigated a number of multiple (mostly doublet) Type IIs. They suggest that the source of the first-component Type II may be generated by flare or by CME, whereas the second-component Type II may be caused by CME front and/or flank. So, to resolve this controversy, the sources of coronal shock have to be further investigated (Vršnak and Cliver, 2008).

In this paper we considered a relatively large sample of 147 Type II events observed between January 1997 and December 2006. Our main goal is to study properties of flares and CMEs associated with these events, aiming to get an insight into the characteristics of flare/CME events causing coronal shocks. Out of many Type II events reported during the period 1997 – 2006 in the *Solar Geophysical Data* (ftp://ftp.ngdc.noaa.gov/STP/SOLAR_DATA/SOLAR_RADIO/SPECTRAL) by the Culgoora Observatory, we have selected a sample of 147 Type II radio bursts on the basis of the following criteria:

i) the starting time, ending time, starting frequency and ending frequency should be certain;
ii) the starting frequency must be below 500 MHz;
iii) all the Type II events should have both fundamental and harmonic signatures;
iv) the location of the related flare must be identified.

The criteria *i*) – *iii*) are used to select clear events in which the properties of Type IIs can be determined. For example, in cases where the starting frequency is higher than 500 MHz and in cases where only fundamental/harmonic exists, the identification of starting value is not certain. Since the second harmonic of the Type II burst is generally more intense than the fundamental, and the ending frequency of the fundamental band is often below the ionospheric cut-off frequency, we only considered events for which both fundamental and harmonic emissions were observed. In addition, most of the Type II bursts occur within 30 – 300 MHz (Nelson and Melrose, 1985) and we have considered an upper limit to the starting frequency as 500 MHz. The associated flares and CMEs were identified on the basis of temporal relationship, *i.e.*, by using a time window of $+/-$ 30 minutes for flares and a time window of 60 minutes before the first detection of CMEs by the LASCO-C2 (http://cdaw.gsfc.nasa.gov) (Brueckner *et al.*, 1995).

Table 1 Properties of Type II radio bursts.

Groups		Starting frequency (MHz)	Shock speed ($km\,s^{-1}$)	Bandwidth (MHz)	Duration (minutes)	Drift rate ($MHz\,s^{-1}$)
Group I	Average	175	871	126	10	0.25
(88 events)	(Median)	(175)	(800)	(112)	(10)	(0.19)
	Standard deviation	76.41	421	73.68	5.83	0.19
Group II	Average	175	698	108	9	0.28
(59 events)	(Median)	(160)	(650)	(90)	(9)	(0.16)
	Standard deviation	85.96	236	71.5	5.32	0.30

We have classified these 147 events into two groups: Group I, representing the events where the onset of Type II must be within the associated flare's impulsive phase (88 events); Group II, representing Type IIs that started during the associated flare's decaying phase (59 events). Note that none of the considered Type II bursts started during the flare precursor phase.

2. Results

2.1. Type II Bursts

The duration (T_d), drift rate, bandwidth, starting frequency (F_s), ending frequency (F_e), and the related shock speed (estimated using Newkirk's density model, Newkirk, 1961) are examined and their distributions are presented in Figure 1a – f, respectively. As seen in these plots, there is no difference between Group I and Group II Type IIs.

A summary of the average and median values of the Type II burst properties are given in Table 1. Inspecting Table 1, one finds that there are practically no differences in starting frequencies, durations, and drift rates of Type IIs of Group I and II. The difference of mean bandwidths is of very low statistical significance, $P = 85\%$. The only statistically significant difference ($P > 99\%$) is found for shock speeds.

Finally, we correlated the basic properties of Type IIs: starting frequency and drift rate, starting frequency and shock speed, starting frequency and duration of Type IIs, to establish empirical relationships between these parameters. The results are presented in Figure 2, showing that there are no significant differences between Group I and Group II Type IIs. In both Groups the only statistically significant correlation ($P > 99\%$) is found between the drift rate and the starting frequency.

2.2. Properties of the Associated Flares

Next, we have studied properties of soft X-ray flares associated with the two classes of Type IIs; their distributions are shown in Figure 3. The statistical properties are summarized in Table 2. It can be seen that there are significant differences between the flare distributions for the two classes. For example, the Group I events are associated with flares of significantly longer durations, rise times, and decay times ($P > 99\%$).

Furthermore, Group I flares are, on average, stronger, since more M-class flares are found in Group I than in Group II, where there are more C-class flares (Figure 3b).

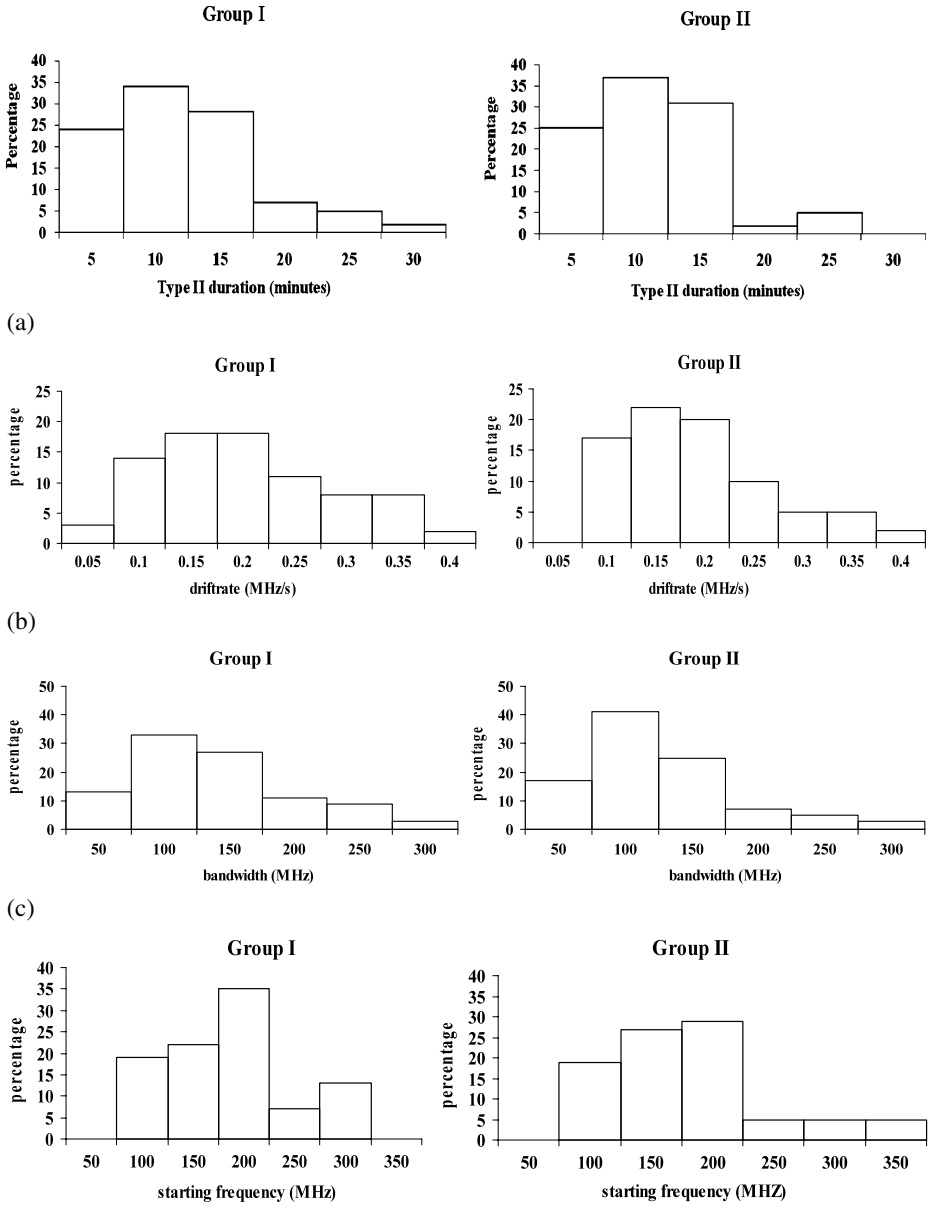

Figure 1 (a) Distribution of Type II duration in Group I and Group II. (b) Distribution of Type II drift rate in Group I and Group II. (c) Distribution of Type II bandwidth in Group I and Group II. (d) Distribution of Type II starting frequency in Group I and Group II. (e) Distribution of Type II ending frequency in Group I and Group II. (f) Distribution of Type II shock speed in Group I and Group II.

In Figure 4 the distribution of delays between Type II and flare start are shown. In both the classes, the delay is the same on average. The delay time between Type II start and flare peak time are shown in Figure 5. In the left panel delay times (Type II start – flare peak)

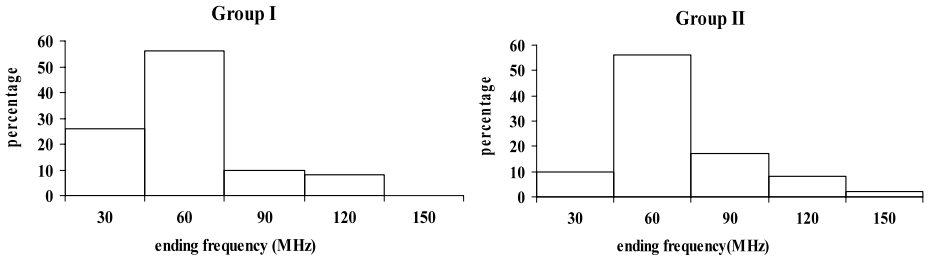

(e)

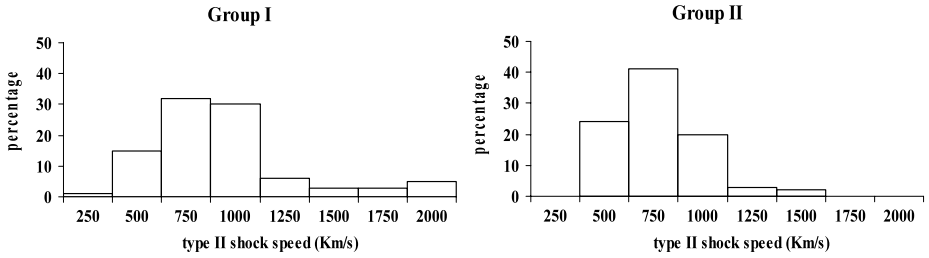

(f)

Figure 1 (*Continued*)

Table 2 Properties of solar flares.

Groups		Type II onset time – flare onset time (minutes)	Type II onset time – flare peak time (minutes)	Flare rise time (minutes)	Flare decay time (minutes)	Flare duration (minutes)
Group I	Average	11	−7.8	19	16	36
(88 events)	(Median)	(9)	(−6)	(16)	(14)	(33)
	Standard deviation	7.5	8.4	11.5	10.99	20.2
Group II	Average	12	2.6	10	10	20
(59 events)	(Median)	(10)	(1)	(8)	(8)	(17)
	Standard deviation	7.0	3.6	7.7	8.5	13.5

are negative, because Type IIs in this group of Type II bursts, by selection, occur before the flare peak time. Analogously, all delays are positive in the right panel. For Group I the distribution peaks at the −5 minutes bin and in Group II most of events are found in the range from 0 to +5 minutes.

Next, we studied the correlations between the properties of Type II bursts and the properties of flares. The results are shown in Figures 6a and 6b. For example, the strong correlation ($P > 99\%$) between the flare rise time and the delay of the Type II onset after the flare beginning is clear from Figure 6a. A weak anti-correlation between the flare rise time and starting frequency of Type II bursts is seen in Figure 6b. The power-law fits in Figure 6b are characterized by the statistical significances $P > 96\%$ and $P > 99\%$ for Group I and Group II, respectively. A similar anti-correlation was found by Vršnak (2001). Note that both groups of Type II exhibit similar relations with flare rise time.

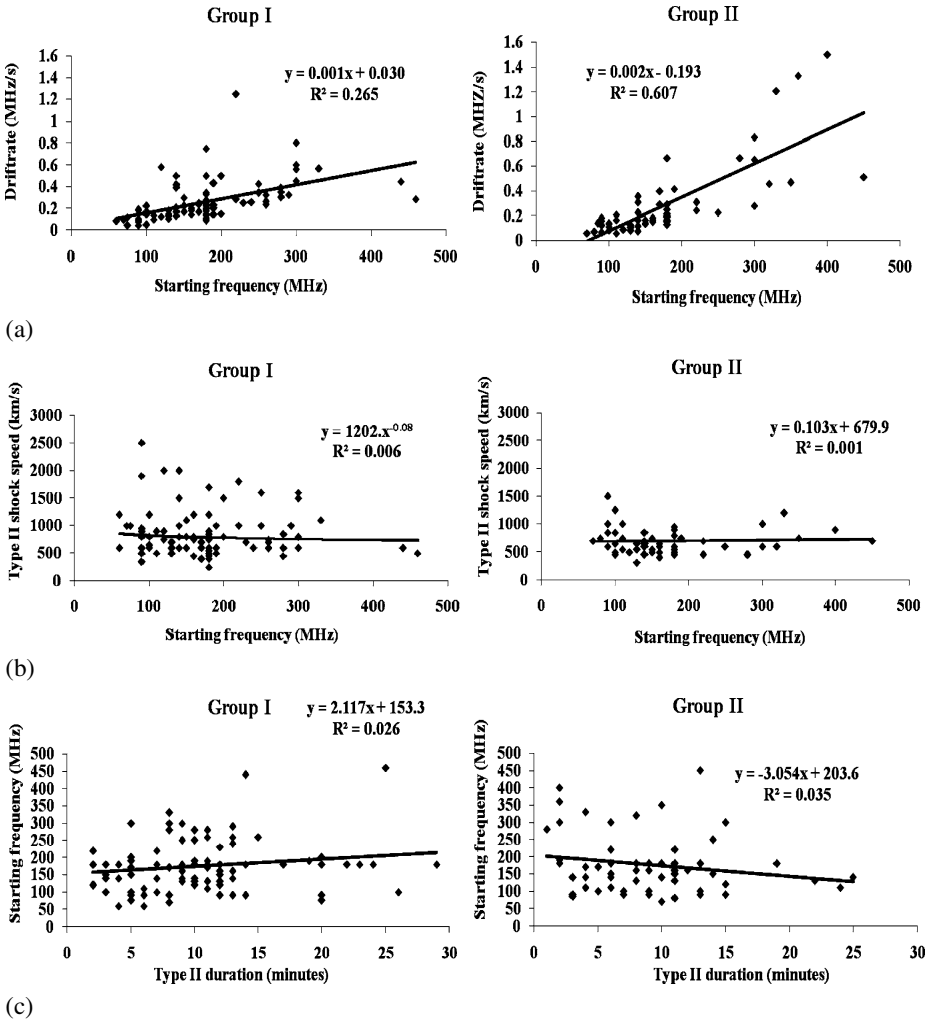

Figure 2 Correlation between (a) starting frequency and drift rate of Type IIs; (b) starting frequency and shock speed of Type IIs; (c) Type II duration and starting frequency in Groups I and II (left and right columns, respectively).

2.3. Association with CMEs

For 77 events out of 88 Group I Type II bursts, there are associated CMEs (no CME reports for 11 cases due to SOHO data gaps) and 45 events out of 59 Group II Type II bursts (no CME reports for 14 cases). The average CME speed was 806 km s^{-1} for Group I sample, in contrast to 536 km s^{-1} for Group II sample. The distribution of time differences between the start of Group I Type II and Group II Type II bursts and the onset of CMEs are shown in Figure 7. The onset time of CMEs at one solar radius was determined using the constant-speed back-extrapolation method and listed in the online LASCO catalog. For Group I Type II bursts, the distribution of time differences between the Type II start and the CME onset peaks at +10 min. For the Group II Type IIs, the distribution peaks at +20 min.

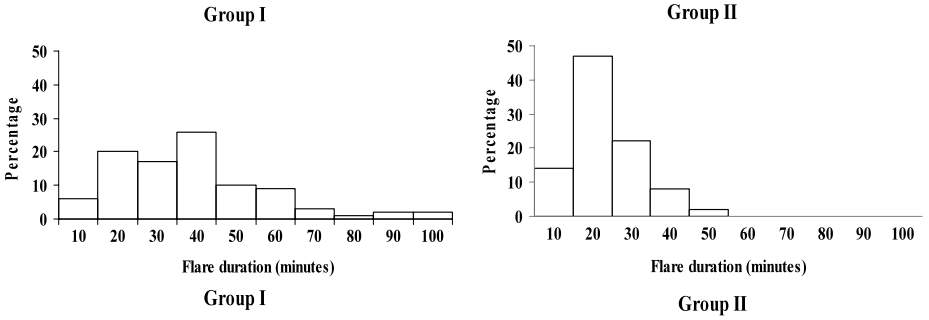

(a)

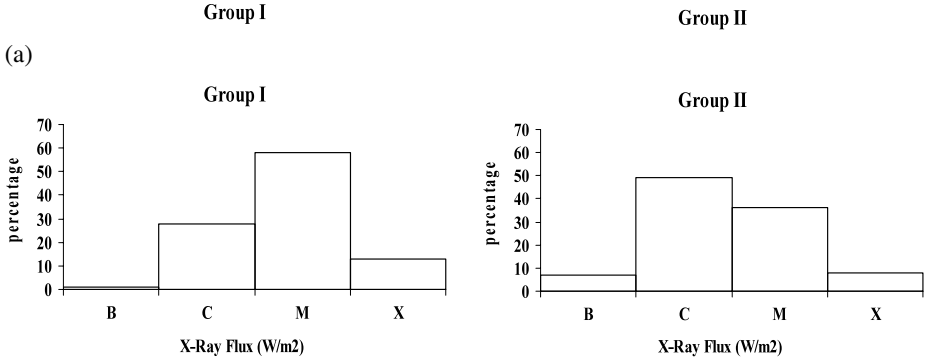

(b)

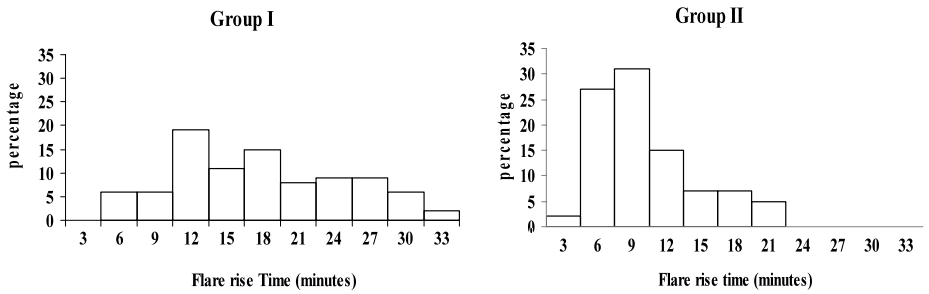

(c)

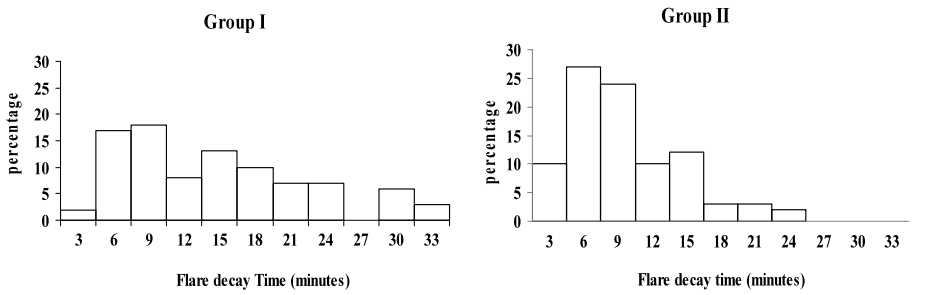

(d)

Figure 3 Distribution of (a) soft X-ray flare durations; (b) soft X-ray peak-fluxes; (c) soft X-ray flare rise times; (d) soft X-ray flare decay times in Groups I and II (left and right column, respectively).

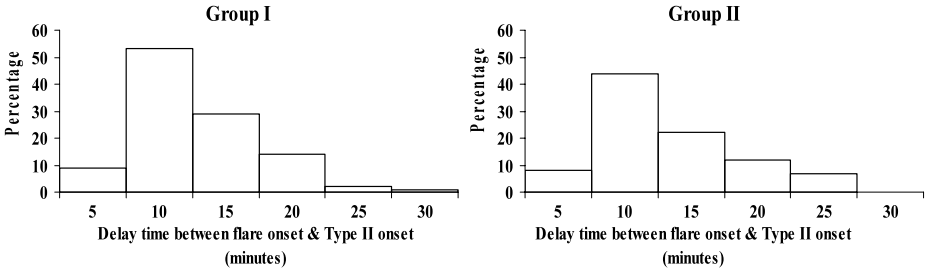

Figure 4 Delays of the Type II burst onset after the flare onset in Group I and Group II.

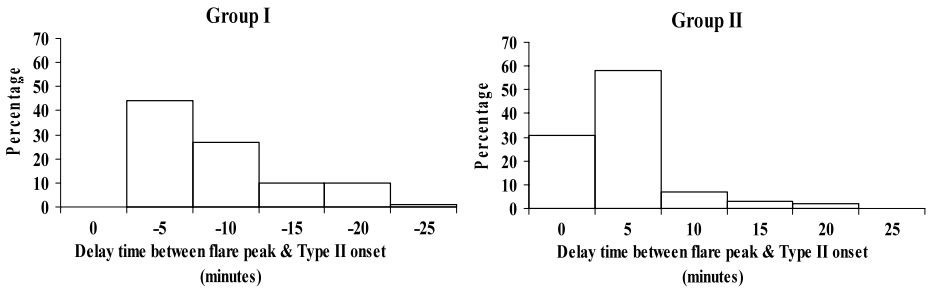

Figure 5 Delays of the Type II burst onset after the flare peak in Group I and Group II.

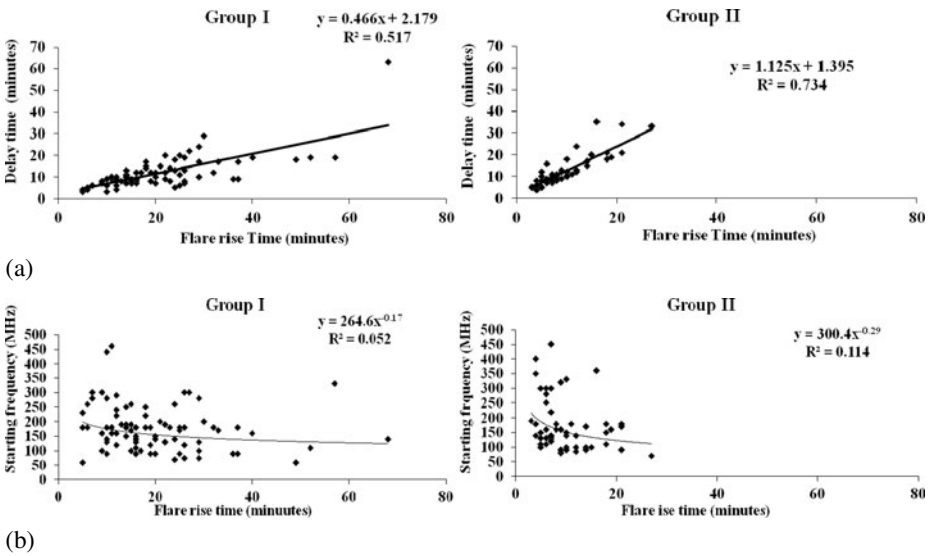

Figure 6 (a) Correlation between flare rise times and the delay of the Type II onset after the flare onset for Group I and Group II. (b) Correlation between flare rise times and the Type II starting frequencies in Group I and Group II.

This difference does not seem to be a significant one due to the following. The CME onset time is the most basic parameter to investigate the relation between flares and CMEs. In

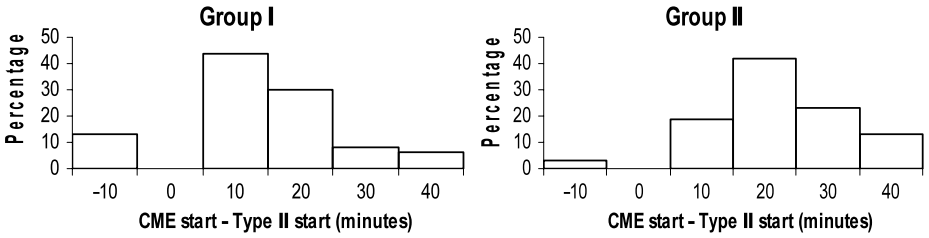

Figure 7 Delay of Type II start after the CME onset in Group I and Group I.

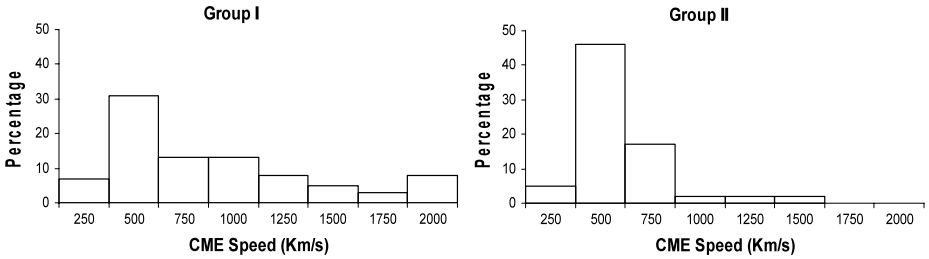

Figure 8 Distribution of CME speeds associated with Group I and Group II.

physical sense, the onset time of a CME should be defined as the beginning of the acceleration phase (see, *e.g.*, Vršnak *et al.*, 2007, and references therein). However, the onset time defined in this manner is difficult to measure since CMEs originate below the LASCO C2 field of view (FOV). It can be estimated only if there are low-coronal signatures of the CME, *e.g.*, expanding EUV structures, or eruptive prominences. Unfortunately, such data are not available for most of the CMEs. Thus, in statistical studies the CME onset is most often estimated by the linear back-extrapolation of the CME trajectory measured in the LASCO C2 and C3 FOV to the solar surface. Such a method obviously has a serious drawback since it does not take into account the effect of the CME acceleration (see, *e.g.*, Harrison and Sime, 1989; Harrison *et al.*, 1990). This can lead to an erroneous estimate of the onset time, especially in the case of gradual CMEs whose acceleration is prolonged into the LASCO C2 and C3 FOVs. However, the situation is much better in the case of fast CMEs, such as those considered in our analysis. In such events the acceleration phase is usually short, which reduces the errors. Furthermore, there are two effects that compensate each other. The presence of the acceleration phase implies that the back-extrapolated onset time should be delayed with respect to the real start of the acceleration phase. On the other hand, CMEs are launched from $R > 1$, *i.e.*, the erupting structure is characterized by some initial height, which compensates the previously mentioned delay. Interplay of these two effects reduces the error of the back-extrapolated onset time, so that for fast CMEs it is typically within 10 min (see Figure 4 in Maričić *et al.*, 2004, or Figure 2 in Vršnak *et al.*, 2007).

Figure 8 shows the distribution of the CME velocities. For CMEs associated with Group I Type IIs, the speeds of CMEs vary from 250 to 2000 km s^{-1}. The mean value is 806 km s^{-1} with standard deviation 571 km s^{-1}. We have found that the CME speed is weakly correlated ($R = 0.35$; $P > 99\%$) with the estimated shock speed of Class I Type IIs (Figure 9, left panel). For CMEs associated with Group II Type IIs the CME speeds vary from 250 km s^{-1} to 1000 km s^{-1}. Compared to CMEs associated with Group I, the mean velocity is significantly lower for Group II (536 km s^{-1} with standard deviation 234 km s^{-1}) and most of

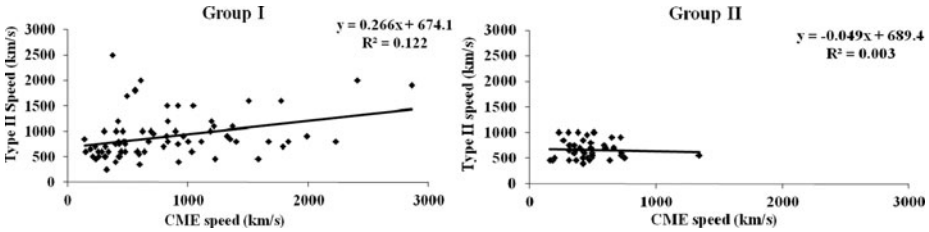

Figure 9 Correlation between CME speeds and Type II speeds for Group I and Group II.

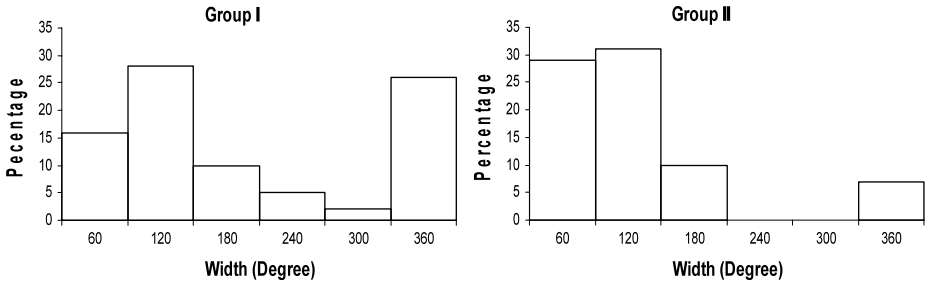

Figure 10 Distribution of CME widths in Group I and Group II.

these CMEs have speeds lower than 900 km s^{-1}. For this Group II, in contrast to Group I, the CME velocities are not correlated at all with the estimated shock speed (Figure 9, right panel). Note that also Type II burst shocks are faster in Group I than in Group II ($P > 99\%$; see Table 1).

Most of the CMEs from our sample decelerate, with mean acceleration around -10 m s^{-2} for both Group I and Group II samples. This is similar to the value of -5 m s^{-2}, found by Lara *et al.* (2003), who also considered CMEs associated with metric Type II radio bursts. The CME widths associated with metric Type II bursts are found in the range between 50 and 360 degrees (Figure 10). In particular, 26% of Group I events were halo CMEs (360 degree width), in contrast to Group II sample, where we find only 7% of halo CMEs.

3. Discussion and Conclusion

Though the two classes of Type IIs appear at different phases of their associated flares, the physical properties of both Type II classes tend to be very similar. For example, both have starting frequencies $\sim 150-200$ MHz, duration $\sim 10-15$ min, and drift rate $\sim 0.1-0.3$ MHz s^{-1}. There are only small differences in estimated shock speeds (800 and 700 km s^{-1}) and bandwidths (126 and 108 MHz).

On the other hand, there are significant differences in the associated soft X-ray flares and CMEs of Group I and II. For example, the rise time, decay time, and duration of Group I flares are longer and the peak flux is higher than in the case of Group II. That is, while Group I Type IIs are associated with longer-duration and stronger flares, Group II Type IIs are associated with shorter-duration and weaker flares. So, given the similarity of Type IIs of both classes, it can be concluded that the appearance of shock during or after the impulsive phase is simply a matter of probability, since in the case of longer impulsive phase (*i.e.*, longer rise time) it is more probable that the shock will appear within the flare rise.

This further implies that characteristics of shocks causing Type II bursts do not depend much on the overall properties of the associated flares. The only relevant flare parameter is the flare rise time, which determines the time delay of the Type II after the flare onset (Figure 6a) and to a certain degree its starting frequency (Figure 6b). This means that Type II bursts associated with more impulsive flares have shorter delays and higher starting frequencies, *i.e*. the shock is formed sooner and at lower heights (see also Vršnak, 2001 and Vršnak, Magdalenić, and Aurass, 2001). Note that such a relationship is consistent with the relationship between the acceleration phase of the source-region expansion and the time/distance needed for the shock formation (Vršnak and Lulic, 2000 and Žic *et al.*, 2008).

Similar to flares, CMEs of both classes of Type IIs show significant differences. For example, the range of velocities and the mean speed are larger for Group I CMEs, and they are of larger widths on average.

In addition, the distribution of delays between the start of Type IIs and onsets of CMEs in Group I peaks at $\sim$ 10 min (Figure 7, left panel), whereas in Group II, the distribution shows maximum at $\sim$ 20 min (Figure 7, right panel). Given that Group II CMEs are slower, this would imply that the shock-formation time depends on the CME speed, which directly relates shocks to CMEs (for the relation between the driver speed and the time/distance of the shock formation see Žic *et al.*, 2008). Since a faster CME implies also a shorter shock-formation time, the shock-formation height (*i.e*., the Type II starting frequency) should be similar to that of slower CME and longer shock-formation time. This is compatible also with the fact that the shock-formation time is correlated with the duration of the flare impulsive phase (Figure 6a), since the CME acceleration phase is usually synchronized with the flare impulsive phase (Zhang *et al.*, 2001; Shanmugaraju *et al.*, 2003; Maričić *et al.*, 2004, 2007; Temmer *et al.*, 2008; for the relationship between the driver acceleration and the time/distance of the shock formation see Žic *et al.*, 2008). In this respect, we note that Group I Type IIs are somewhat faster than Group II Type IIs, consistent with higher CME speeds in Group I sample. However, lack of clear correlation between the CME speed and the shock speed (Figure 9) implies that at least a fraction of Type II burst shocks are caused by flares, degrading the CME-speed/shock-speed correlation, while not affecting the relationship between the flare rise time and the shock-formation time and starting frequency.

Acknowledgements We sincerely thank the referee for his/her constructive suggestions on the manuscript. We are grateful to the Solar Geophysical Data team for their open data policy. The CME catalog we have used is generated and maintained by the Center for Solar Physics and Space Weather, The Catholic University of America in cooperation with the Naval Research Laboratory and NASA. SOHO is a project of international cooperation between ESA and NASA.

References

Aurass, H.: 1997, In: Trottet (ed.) *Coronal Physics from Radio & Space Observations*, *Lecture Notes in Physics* **483**, Springer, Berlin, 135.

Brueckner, G.E., Howard, R.A., Koomen, M.J., Korendyke, C.M., Michels, D.J., Moses, J.D., Socker, D.G., Dere, K.P., Lamy, P.L., Llebaria, A., *et al.*: 1995, *Solar Phys.* **162**, 357.

Cliver, E.W.: 1999, *J. Geophys. Res.* **104**(A3), 4629.

Gopalswamy, N.: 2000, In: Stone, R.G., *et al.* (eds.) *Geophys. Monogr.* **119**, AGU, Washington, 123.

Gopalswamy, N., Kaiser, M.L., Lepping, R.P., Kahler, S.W., Ogilvie, K., Berdichevksy, D., Kondo, T., Isobe, T., Akioka, M.: 1998, *J. Geophys. Res.* **103**, 307.

Gopalswamy, N., Lara, A., Kaiser, M.L., Bougeret, J.L.: 2001a, *J. Geophys. Res.* **106**(A11), 25261.

Gopalswamy, N., Yashiro, S., Kaiser, M.L., Howard, R.A., Bougeret, J.L.: 2001b, *J. Geophys. Res.* **106**(A12), 29219.

Harrison, R.A., Sime, D.G.: 1989, *Astron. Astrophys.* **208**, 274.

Harrison, R.A., Hildner, E., Hundhausen, A.J., Sime, D.G., Simnett, G.M.: 1990, *J. Geophys. Res.* **95**, 917.

Lara, A., Gopalswamy, N., Nunes, S., Muoz, G., Yashiro, S.: 2003, *Geophys. Res. Lett.* **30**, 8016. doi:10.1029/2002GL016481.
Mann, G., Classen, T., Aurass, H.: 1995, *Astron. Astrophys.* **295**, 775.
Maričić, D., Vršnak, B., Stanger, A.L., Veronig, A.M.: 2004, *Solar Phys.* **225**, 337.
Maričić, D., Vršnak, B., Stanger, A.L., Veronig, A.M., Temmer, M., Roša, D.: 2007, *Solar Phys.* **241**, 91.
Nelson, G.J., Melrose, D.B.: 1985, In: McLean, D.J., Labrum, N.R. (eds.) *Solar Radiophysics*, Cambridge University Press, Cambridge, 350.
Newkirk, G.A.: 1961, *Astrophys. J.* **133**, 983.
Reiner, M.J., Kaiser, M.L., Gopalswamy, N., Aurass, H., Mann, G., Vourlidas, A., Maksimovic, M.: 2001, *J. Geophys. Res.* **106**, 25279.
Shanmugaraju, A., Moon, Y.H., Dryer, M., Umapathy, S.: 2003, *Solar Phys.* **215**, 161.
Shanmugaraju, A., Moon, Y.J., Cho, K.S., Kim, Y.H., Dryer, M., Umapathy, S.: 2005, *Solar Phys.* **232**, 87.
Smerd, S.F., Sheridan, K.V., Stewart, R.T.: 1975, *Astrophys. Lett.* **16**, L23.
Subramanian, K.R., Ebenezer, E.: 2006, *Astron. Astrophys.* **451**, 683.
Temmer, M., Veronig, A.M., Vršnak, B., Rybak, J., Gomory, P., Stoiser, S., Maričić, D.: 2008, *Astrophys. J.* **673**, L95.
Uchida, Y.: 1960, *Publ. Astron. Soc. Japan* **12**, 376.
Vršnak, B.: 2001, *J. Geophys. Res.* **106**, 25291.
Vršnak, B., Lulic, S.: 2000, *Solar Phys.* **196**, 181.
Vršnak, B., Cliver, E.W.: 2008, *Solar Phys.* **253**, 215.
Vršnak, B., Magdalenić, J., Aurass, H.: 2001, *Solar Phys.* **202**, 319.
Vršnak, B., Ruždjak, V., Zlobec, P., Aurass, H.: 1995, *Solar Phys.* **158**, 331.
Vršnak, B., Maričić, D., Stanger, A.L., Veronig, A.M., Temmer, M., Rosa, D.: 2007, *Solar Phys.* **241**, 85.
Wild, J.P., McCready, L.L.: 1950, *Aust. J. Sci. Res. A* **3**, 387.
Zhang, J., Dere, K.P., Howard, R.A., Kundu, M.R., White, S.M.: 2001, *Astrophys. J.* **559**, 452.
Žic, T., Vršnak, B., Temmer, M., Jacobs, C.: 2008, *Solar Phys.* **253**, 237.